

# Investigating the Behavior of Coupled Steel Plate Shear Wall under Cyclic Loading

Behzad Haseli<sup>1</sup> · Farzad Azarmi Alimohammadi<sup>2</sup> · Ehsan Adili<sup>3</sup> · Saeed Rasekh<sup>4</sup> · Meysam Mardi<sup>5</sup>

Received: 19 April 2021 / Accepted: 1 April 2022 / Published online: 4 May 2022  
© The Institution of Engineers (India) 2022

**Abstract** Using resistant systems in construction industry is essential to reduce the damages caused by earthquake loads. One of the most suitable resistant systems is steel plate shear wall with a coupling beam (Coupled Steel Plate Shear Wall or CSPSW), which comprises horizontal boundary elements (beams), vertical boundary elements (columns) and steel plate. In this study, the behavior of CSPSW under the effect of cyclic loading in three (six-, eight- and twelve-story) frames for three different lengths of coupling beam has been investigated in OpenSees. In the first part of this study, the structure responses including shear capacity, flexural capacity, energy dissipation, ductility of shear wall and coupling beam, and rotation created in coupling beam are investigated. The results indicated that the effect of coupling beam length on the performance of the components of the CSPSW is different, in a way that as the coupling beam length is increased, the shear capacity, flexural capacity, energy dissipation and ductility of coupling beam increase, and its maximum displacement reduces. However, as the coupling beam length is increased, the shear capacity, flexural capacity, energy dissipation and ductility of shear wall decrease and its maximum displacement increases. It was also found that as the frame height increases, the rate of increase in shear force and the bending moment in shear wall grow higher

than those of coupling beam. In the second part of this study, the shear capacity equation related to the CSPSW is rewritten and proposed based on the variable ‘coupling beam length’.

**Keywords** Coupled steel plate shear wall · Cyclic load · Energy dissipation · Ductility · Shear capacity equation

## Introduction

Large earthquakes in near-fault and far-fault cities are inevitable to occur. If these earthquakes are under the influence of progressive orientation, certain pulses can be seen in the displacement and velocity time-history seismic records, affecting the structure strongly and rapidly [1]. One of the most common resistant systems against lateral forces, as an economical and easy-to-implement option, is coupled steel plate shear walls. The advantages of steel plate shear walls include high ductility, high energy absorption, high initial shear stiffness, and resolving the limit of span length-to-depth ratio less than two [2], in similar concrete samples [3]. In the event of an earthquake, the lateral forces applied to the coupled steel plate shear wall system create an axial force in the walls and then this axial force creates large shear forces in coupling beams. Therefore, the coupling beams improve the behavior of the frame against overturning moment. It should be noted that very strong coupling beams produce large forces in walls, causing the shear wall to fail before the coupling beam. On the other hand, if the coupling beam is weakly designed, in ultimate condition, the coupling beams will fail before the shear wall and dissipate the seismic energy alone. Therefore, accurate knowledge about the behavior of the coupling beam and shear wall in the coupled steel plate shear

✉ Behzad Haseli  
b.haseli@yahoo.com

<sup>1</sup> Faculty of Engineering, Kharazmi University, Tehran, Iran

<sup>2</sup> Islamic Azad University, Qazvin Branch, Qazvin, Iran

<sup>3</sup> Faculty of Engineering, Velayat University, Iranshahr, Iran

<sup>4</sup> Sadra Institute of Higher Education, Tehran, Iran

<sup>5</sup> Islamic Azad University, Roodehen Branch, Tehran, Iran

wall system brings about a correct understanding of the system performance and improves its design process [4]. Therefore, the performance of the components of the coupled steel plate shear wall (steel plate shear wall and coupling beam) under the effect of cyclic load is investigated in this study, and then the shear capacity equation of the coupled steel plate shear wall, based on the coupling beam length, is presented. Mazaheri et al. [5] evaluated the performance of coupled steel plate shear wall with reduced-cross-section boundary beam in a study. This study was conducted numerically using the analyses done by Abaqus. Based on the results, it was found that using reduced-cross-section beams in coupled steel plate shear wall increases 2 to 17 percent out-of-plane buckling, reduces shear capacity by 6 to 20 percent, and reduces energy dissipation by 6 to 71 percent, compared to the sample without reduction in cross section. Hoehler et al. [6] conducted a study on six samples of 2.7 m × 3.7 m gypsum-coated shear walls consisting of cold-rolled steel plate sheets that were exposed to earthquake and fire loads. The results of this study showed that the use of gypsum-coated steel plate shear wall reduces by 35% the lateral bearing capacity caused by deformation in the case of wall failure due to local buckling, compared to the wall not exposed to fire. Pavir and Shekastehband [7] investigated the hysterical behavior with eight four-story models with different sizes of cross section and coupling beam length. The ratios of beams with shear and flexural failure modes are less than 1.6 and more than 2.6, respectively. The results of this study indicated the significant contribution of coupling beams to the absorption of energy into structural system. Hu et al. [8] evaluated the deformation capacity of a concrete-filled composite shear wall. They could develop an analytical program to analyze the bending moment behavior of concrete-filled composite steel plate shear wall. The program was based on cross-section analysis of fiber using refined materials model. The accuracy of the program, in comparison with the existing laboratory results, has been investigated. The results led to proposing a simplified formula based on the input of materials and geometry, which has been defined in order to calculate the final curvature associated with 15% drop in the moment capacity. Dan et al. [9] conducted a study entitled ‘theoretical and experimental study on composite steel–concrete shear walls with vertical steel-encased profiles. In buildings that require high lateral bearing capacity, Composite steel–concrete structural shear walls with steel-encased profiles can be used as resistant systems against horizontal forces. They could evaluate the maximum load, deformation capacity and dissipated energy using experiments. Fahnestock and Borello [10] conducted extensive studies on the behavior of coupled steel plate shear walls with coupling beams. In a study, these researchers investigated the

behavior of steel plate shear walls with different lengths of coupling beams in OpenSees. The results showed that the shear strength and the drift of primary layers increase as the length of the coupling beam goes up [11]. Berman et al. [12] conducted a study to compare the cyclic behavior of shear walls and bracing frames. In this study, the cyclic behavior and energy absorption of steel frames with bracing systems, and the smooth and corrugated shear walls were studied and evaluated. Based on the results, it was observed that the braced frame has the most initial stiffness compared to other frames, and that the smooth shear wall has the highest ductility. Ghadaksaz et al. [13] investigated the effect of the parameters of coupling beam on steel plate shear wall and evaluated samples of coupling beams with different number of story and different lengths. The results showed that with increasing the length of the coupling beams in the steel shear wall, the shear strength of the shear wall decreases. Safari Gorji and Cheng [14–16] compared the seismic performance of such C-SPSW systems with that of C-SPSWs with rigid frames. They designed and analyzed several prototypes using a series of nonlinear response history and pushover analyses. It is observed that the simple boundary frames C-SPSWs exhibited more satisfactory seismic performance in compare with C-SPSWs with rigid frames under both 10.50 and 2.50 hazard levels, while fabrication cost was reduced. It can be seen that significant studies have been done to investigate the behavior of coupled steel plate shear wall, but no comparison has been made between the components of coupled steel plate shear wall (steel shear wall and coupling beam) in terms of their performances. Therefore, in the present study, shear capacity, flexural capacity, ductility and energy dissipation of coupling beam and steel shear wall in the system of coupled steel plate shear wall under cyclic load are investigated, and the equation of shear capacity in coupled steel plate shear wall based on the parameter ‘coupling beam length’ is provided.

### Designing Coupled Steel Plate Shear Walls with Coupling Beam

The US Code AISC/ANSI-341-16[17] introduced the criteria for designing the coupled steel plate shear walls in 2010 (ASCE) [18]. It should be noted that steel shear walls are called Steel Plate Shear Walls (SPSW) in this Code. The columns are also referred to as Vertical Boundary Elements (VBE), the beams as Horizontal Boundary Elements (HBE) and the steel plate as Web Plate. In this Code, the nominal resistance of web plate is obtained from Eq. (1).

$$V_n = 0.42F_y t_w l_{cf} \sin 2\alpha \quad (1)$$

In Eq. (1),  $F_y$  and  $t$ , respectively, are the yield stress and

the thickness of steel plate.  $L_{cf}$  is the distance between the flanges of VBE, and  $\alpha$  is the angle of tensile field. According to this Code, the existing shear strength of web plate is expressed as  $\phi V_n$  where  $\phi = 0.9$  based on LRFD Method, and as  $V_n/\Omega$  where  $\Omega = 1.67$  based on ASD Method. When the steel plate shear walls are designed using certain seismic parameters, the designing criterion should be such that the system has significant ductility and sufficient additional strength. To achieve such performance, the ductile rupture modes must first occur before that the brittle rupture modes begin in the non-gravitational bearing elements of system, and then, if necessary, the gravitational bearing elements expand at the end of the earthquake in a controlled pattern in which no progressive collapse occurs [19].

The structural behavior of coupled steel plate shear wall system against reciprocating load changes as the coupling degree presented in Eq. (2) changes. Thus, if the coupling degree is equal to 0%, the two side shear walls behave separately, and if the coupling degree is equal to 100%, the bases of two side shear walls act as a single base, and in this condition, the formation of paste joint (plastic hinge in joint) in the wall before the beam threatens the structure safety. Therefore, it is necessary for the coupling degree (CR) to be such that first, the paste joint is formed in the coupling beam. In Eq. (2),  $V_{BEAM}$  is the shear strength of coupling beam,  $L$  is the distance from center to the center of wall base, and  $m_i$  is the flexural strength of wall base.

$$CR = \frac{L \sum V_{BEAM}}{L \sum V_{BEAM} + \sum m_i} \quad (2)$$

Based on the results of previous studies, the coupling degree of coupled shear wall with coupling beam is recommended to be between 30 and 45% [20]. Therefore, in the present study, the pairing ratio was 35%. In Fig. 1, the coupling of coupled steel plate shear walls and the

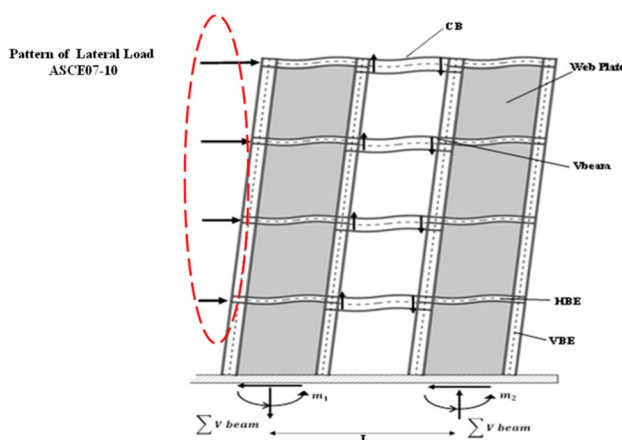


**Fig. 1** Coupling and the components of the coupled steel plate shear wall and pattern of lateral load

pattern of lateral loading in the height of the frames can be seen.

### Modeling the Coupled Steel Plate Shear Wall in OpenSees

Equivalent diagonal steel elements have been used to model the behavior of steel plate shear walls based on the method proposed by Kulak et al. [21]. In this method, the tensile field of shear wall filler plate is replaced with steel diagonal plates, and the equivalent diagonal rods, due to the joint connection of their two ends, can only withstand the main tensile stresses. Therefore, after selecting a set of diagonal plates, the equivalent thickness is determined and an equivalent diagonal element is modeled by connecting the two ends of the joint. On the other hand, due to the two-dimensional modeling in the present study, obtaining the information of the dominant buckling mode is important. Therefore, modeling the equivalent diagonal element simulates the buckling mode behavior well.

In the present study, the nonlinear behavior of shear walls is modeled using fiber sections that can be used to define the cross section of each element. For this purpose, the behavior of each element is defined by assembling the stress–strain diagrams of the meshes of that element, each of which reflects the mechanical and behavioral properties of steel materials. These elements are connected in parallel and the overall behavior of a steel wall is modeled. Therefore, cyclic materials were used for modeling the steel plate shear walls, according to the Hysteretic Uniaxial Material command which is used for making two-line cyclic uniaxial materials with force thinning and deformation, malfunction due to ductility and energy, and reduced loading hardness based on ductility. Figure 2 shows the stress–strain curve of cyclic materials.  $K_0$  is initial stiffness, and beta is a power used to determine the degraded unloading stiffness based on ductility ( $M_u - \beta$ ) [22]. For modeling the behavior of coupling steel beam, according to Fig. 3, a beam with elastic cross

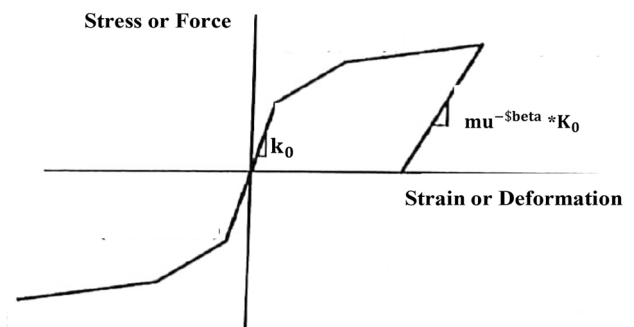


**Fig. 2** Stress–strain curve of cyclic materials used in modeling the coupled steel plate shear walls [22]

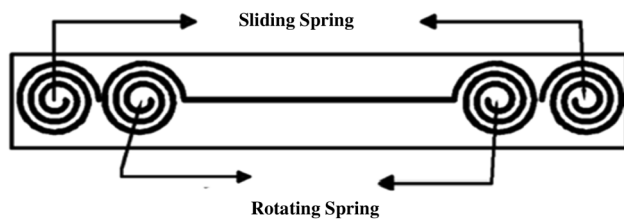


**Fig. 3** Elastic beam model with rotating and sliding hinge for modeling the coupling beam

section with specific bending and shear stiffness is used to calculate linear deformations, and a nonlinear rotational spring is utilized at each end of the beam to consider the bending and shear deformations. As can be seen in Fig. 3, a rotational elastic spring is used to consider the sliding deformations. The tensile stiffness of the coupling steel beams is obtained from Eqs. (3) and (4) proposed by Harris et al. [23, 24].

$$EI_{\text{eff}} = 0.6k'E_sI_{gs} \quad (3)$$

$$k' = \left(1 + \frac{12E_sI_{gs}\lambda}{L_c^2G_sA_w}\right)^{-1} \quad (4)$$

In these equations,  $k'$  is the decrease in the flexural stiffness due to shear deformations,  $I_{gs}$  is the cross-section inertia moment,  $E_s$  is the elasticity modulus of steel,  $G_s$  is the shear modulus of steel,  $A_w$  is the cross-sectional area of shearing resistant steel,  $\lambda$  is the shearing coefficient, and  $L_c$  is the effective span of coupling beam.

### Studied Samples

The present study included three six-, eight-, and twelve-story and three-spans 2D frames with three different lengths of coupling beam, and the coupling beams were 1.65, 3.5 and 5 m long (study is confined to 2D frames only and all frames in this study are structurally, geometrically and loadingly similar to the models proposed in Reference 7). All stories were 4 m high, and the two side spans in all frames were 3.2 m long. The length of middle span of frame also varies according to the length of coupling beam. The dimensions of sections have been obtained via initially designing the three frames in Etabs. Loading was done in accordance with AISC Code [17], and the design seismic lateral load distribution in the height levels of story was according to ASCE07-10 [18] (See Fig. 1). It should be noted that dead and live loads of stories are considered 5 and 3.2 kPa, respectively. Furthermore, the amounts of roof dead and live loads are 3 and 1.5 kPa, respectively. The weight of sections is also obtained by multiplying the cross section by the unit weight of the volume of steel sections. Table 1 presents the evaluated models in this

**Table 1** Introduction of evaluated models in the present study

Abbreviation	Explanation
B6a	Six-story frame with 1.65 m coupling beam
B6b	Six-story frame with 3.5 m coupling beam
B6c	Six-story frame with 5 m coupling beam
B8a	Eight-story frame with 1.65 m coupling beam
B8b	Eight-story frame with 3.5 m coupling beam
B8c	Eight-story frame with 5 m coupling beam
B12a	Twelve-story frame with 1.65 m coupling beam
B12b	Twelve-story frame with 3.5 m coupling beam
B12c	Twelve-story frame with 5 m coupling beam

study. In Table 2, the sections of middle and side columns as well as the coupling beams can be seen. All sections are the result of design in Etabs software. Total height of section (first number), flange width (second number), web plate thickness (third number) and flange thickness (fourth number) have been used for naming the  $I$ -shaped sections of beams ( $I_{\text{first, second, third, fourth number}}$ ). The analysis done in the present study is a static analysis controlled by displacement (nonlinear analysis). Therefore, only the loading pattern matters in such loading. Cyclic loading was applied to structure models up to drift of 5% according to the SAC loading protocol [25], as shown in Fig. 4.

### Results of Modeling

Due to the structural similarity of the frames studied in the present study with the four-story coupled steel plate shear wall presented by Pavir and Shekastehband [7], in order to verify the results presented in this study, the *CSSHL2* hysteresis curve from Pavir and Shekastehband (black curve in Fig. 5) has been examined. In Fig. 5, the envelope hysteresis curve obtained from Pavir and Shekastehband (green curve) is compared with the one obtained from the sample modeled in the present study (red curve). The difference in the results of force–drift hysteresis curve envelope of the studied model can be seen in Table 3. Table 4 presents the numerical parameters for modeling the *CSSHL2* model (Fig. 6).

Loading in this study is cyclic (Fig. 4), and the studied responses are obtained in the form of hysteresis rings in the positive and negative regions. In Figs. 7 and 8, push (cover) of hysteresis curves are shown. In fact, all the responses are reciprocating and the curve cap (push) is drawn. Figure 7 shows the shear force–displacement hysteresis curve envelope obtained from the cyclic analysis of the components of the coupled steel plate shear wall, including the coupling beam, and the steel plate shear wall of six-, eight- and twelve-story frames in different modeling conditions.

**Table 2** Naming the Modeled Frames to Investigate the Behavior of Steel Plate Shear Wall with Coupling Beams

Intended frame	Coupling beam length (m)	Abbreviation	Side column (box section (mm))	Middle column (box section (mm))	Beam of roof (I-shaped (mm))	Beam of story (I-shaped (mm))	Coupling beam (I-shaped (mm))
6story	$L = 1.65$	B6a	Box500 × 500 × 30	Box400 × 400 × 30	1400 × 300 × 8 × 20	1300 × 200 × 6 × 15	1800 × 400 × 15 × 20
	$L = 3.5$	B6b	Box500 × 500 × 30	Box400 × 400 × 30	1400 × 300 × 8 × 20	1300 × 200 × 6 × 15	1800 × 400 × 15 × 20
	$L = 5$	B6c	Box500 × 500 × 30	Box400 × 400 × 30	1400 × 300 × 8 × 20	1300 × 200 × 6 × 15	1800 × 400 × 15 × 20
8story	$L = 1.65$	B8a	Box600 × 600 × 30	Box500 × 500 × 30	1400 × 300 × 10 × 30	1300 × 200 × 6 × 15	1800 × 400 × 15 × 20
	$L = 3.5$	B8b	Box600 × 600 × 30	Box500 × 500 × 30	1400 × 300 × 10 × 30	1300 × 200 × 6 × 15	1800 × 400 × 15 × 20
	$L = 5$	B8c	Box600 × 600 × 30	Box500 × 500 × 30	1400 × 300 × 10 × 30	1300 × 200 × 6 × 15	1800 × 400 × 15 × 20
12story	$L = 1.65$	B12a	Box600 × 600 × 30	Box500 × 500 × 30	1400 × 300 × 10 × 30	1300 × 200 × 6 × 15	1800 × 400 × 15 × 20
	$L = 3.5$	B12b	Box600 × 600 × 30	Box500 × 500 × 30	1400 × 300 × 10 × 30	1300 × 200 × 6 × 15	1800 × 400 × 15 × 20
	$L = 5$	B12c	Box600 × 600 × 30	Box500 × 500 × 30	1400 × 300 × 10 × 30	1300 × 200 × 6 × 15	1800 × 400 × 15 × 20

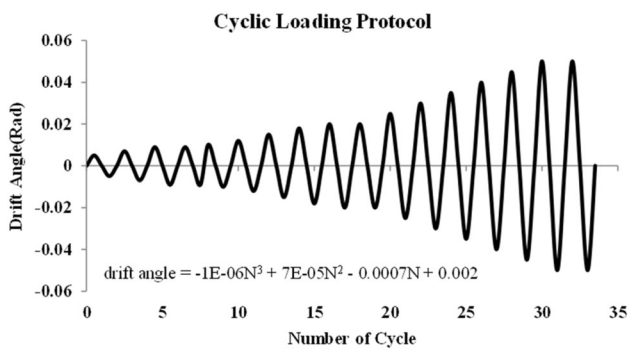


**Fig. 4** The cyclic loading applied to structure [25]

Based on the results obtained, it is observed that with increasing the length of the coupling beam, the shear strength, stiffness (initial slope of diagram) and the

dissipated energy (the area under curve) increase in the coupling beam, and the shear capacity decreases in steel plate shear walls. In the case of six-story frame, for instance, by increasing the length of coupling beam from 1.65 to 3.5 m and then to 5 m, 34 and 53.9% increase can be respectively seen in the shear strength of coupling beam, 18.3 and 25.7% increase in the maximum shear capacity of coupling beam, and 3.2 and 15.8% decrease in the shear capacity of steel plate shear wall. Increasing the length of coupling beam also rises the maximum displacement recorded in steel plate shear wall. In the case of six-story frame, with increasing the length of coupling beam from 1.65 to 3 m and 5 m, the maximum displacement created in the steel plate shear wall has been enhanced from 6.85 to 7.1% and 7.3%, respectively, while increasing the length of coupling beam has reduced the maximum displacement of

**Table 3** Difference between the results of Pavir and Shekastehband [7] with those of the present study

Method	Force (kN)	Roof displacement (cm)
Pavir and Shekastehband [7]	4410	0.050
Present study	4340.98	0.0482
Difference in percentage	1.56	3.6

**Table 4** Numerical parameters for modeling the CSSHL2 model [7]

Intended element	$E$	$F_y$	$F_u$	$F_f$
Beam—column—coupling beam	210.898 MPa	257.2 MPa	–	–
Steel plate shear wall	210.898 MPa	257.2 MPa	344 MPa	277 MPa

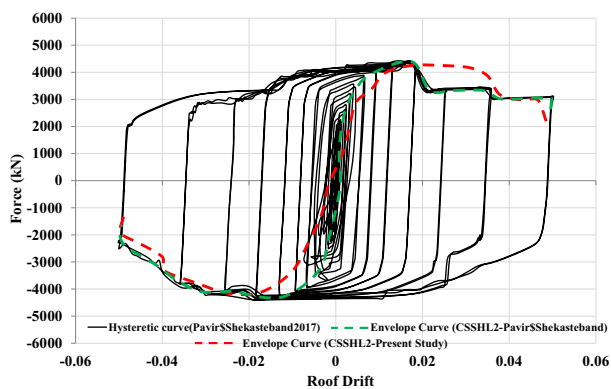


**Fig. 5** Comparison of force–roof drift hysteresis curve three-span four-story frame with steel plate shear walls (CSSHL2)

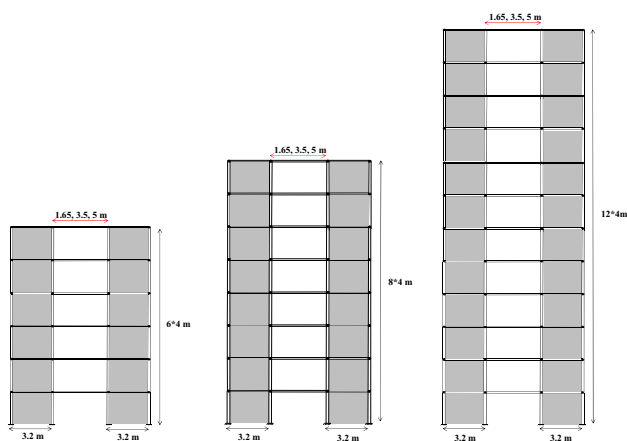


**Fig. 6** Dimensions of models (6, 8 and 12 frame story)

coupling beam. The results show that increasing the height of frame increases the maximum shear force created in coupling beam and steel plate shear wall. In Fig. 8, the bending moment–rotation curve envelope of the components of coupled steel plate shear wall, including the coupling beam and the steel plate shear wall of six-, eight- and twelve-story frames, can be seen. The results show that with increasing the dimensions of coupling beam, the changes of maximum bending capacity have an ascending and descending trend in coupling beam and steel plate shear wall, respectively. In other words, by increasing the length of coupling beam in all the frames under study, the bending capacity of coupling beam increases and the bending capacity of steel plate shear wall decreases. It should be noted that the major part of the flexural capacity of frame is provided by the coupling beam. For example, in an eight-story frame, with increasing the length of coupling beam from 1.65 to 3.5 m and 5 m, 4.46 and 10.34% increase can be seen in the maximum bending capacity of coupling beam, and 12.2 and 18.3% decrease in the bending capacity of steel plate shear wall. Based on the

diagrams presented in Fig. 8, it can be seen that increasing the frame height does not have the same effect on increasing the maximum bending capacity of coupling beam and steel plate shear wall, in a way that the rate of such increase has been achieved to be 20.8% in coupling beam and 40.8% in steel plate shear wall. Increasing the height of frame caused a 12.5% increase and 26% decrease in the maximum rotation recorded in the roof story, respectively, in the coupling beam and the steel plate shear wall. The values of the coupling beam moments ( $M$ ) in Fig. 8, obtained using the corresponding shear forces ( $V$ ) in Fig. 7 using following equation  $M = V \times e/2$ , where  $e$  is the length of the coupling beam.

Figure 9 shows the rotations of coupling beam in different floors of six-, eight- and twelve-story frames for three different lengths of coupling beam. The rotation of coupling beam is obtained based on the displacement created at the end points (points i and j Fig. 9) and is of end rotation type. Based on the results obtained, it can be seen that increasing the length of coupling beam has decrease the rotations created in coupling beam. For example, in case of twelve-story frame, by increasing the length of coupling beam from 1.65 to 3.5 m, we see an average decrease of 7.33% rotations recorded in coupling beam. A 20.66% decrease in rotation has been obtained in 5 m coupling beam, compared to 1.65 m coupling beam. Based on results of White and Adebare [26], increasing the coupling beam length decreases the rotation demand. To investigate the effect of the height parameter of the structure on the rotation of coupling beam, the average rotation of coupling beam in the height levels of the floors in each of the six-, eight- and twelve-story frames has been explored. According to Fig. 9, it can be seen that, in general, the increase in frame height has increased the recorded rotation in coupling beam so that the maximum increase in rotations of coupling beam for  $B(6-8-12)_a$ ,  $B(6-8-12)_b$  and  $B(6-8-12)_c$  models was found to be 20, 33.8 and 39.8%, respectively.

The area below the diagram of the shear force–displacement cycle curve is equal to the numerical value of the energy dissipation, and the maximum displacement to displacement ratio corresponding to the yield shear force is equal to the ductility index. Given that there are three frames with different heights, the values of ductility and energy dissipation in them will not be comparable with each other, Therefore, in order to compare the trend of the energy dissipation and ductility based on the length of the coupling beam, in three frames with different heights, the studied responses have been divided into the largest numerical value of relevant quantity and have been normalized. After that, comparing the energy dissipation and ductility in three frames is possible. Based on the results obtained, it is observed that with increasing the length of

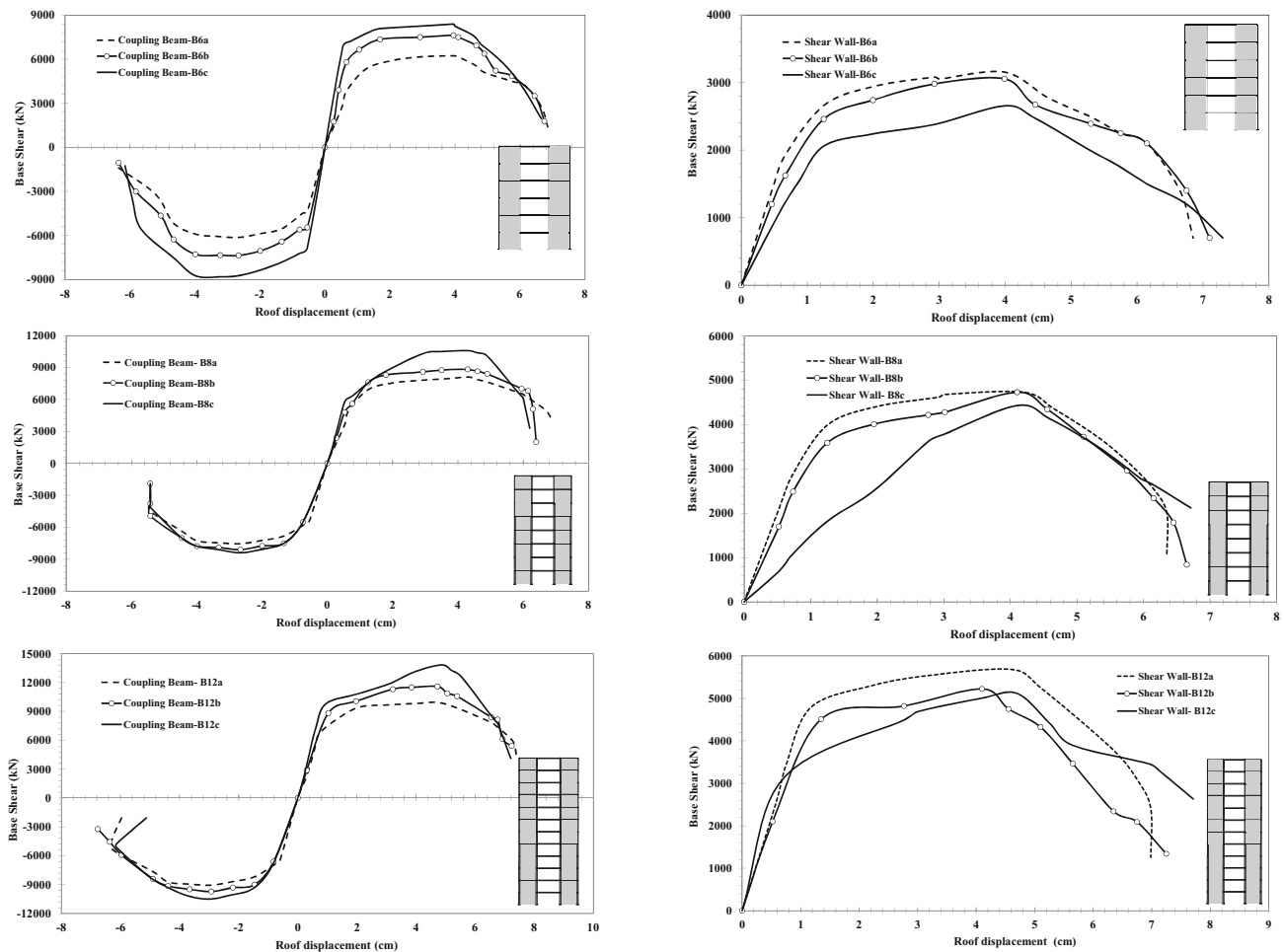


**Fig. 7** Comparison of base shear–displacement hysteresis curve envelope of coupling beam and shear wall of six-, eight- and twelve-story frames in different models

the coupling beam, the energy dissipation in coupling beam and steel plate shear wall has an increasing and decreasing trend, respectively. For example, in a six-story frame, increasing the length of coupling beam from 1.65 to 3.5 m and 5 m has increased the energy dissipation of coupling beam by 18 and 25% and decreased the energy dissipation of steel plate shear wall by 3 and 19%, respectively. Also, increasing the length of coupling beam has increased its ductility so that in a 6 m frame with increasing the length of coupling beam from 1.65 to 5 m, we see a 35% increase in its ductility. To investigate the effect of structure height parameter on ductility and energy dissipation, the average responses of numerical values different from the length of coupling beam have been examined. The responses under study are divided into the largest numerical value of the relevant quantity and are so-called normalized. Figure 10 shows the changes in ductility and normalized energy dissipation of coupling beam, and steel plate shear wall for different height levels of the frames studied. It is observed that with increasing the number of story, the normalized

energy dissipation of coupling beam and steel plate shear wall in the studied frames has an increasing trend. The increase rate of energy in the steel plate shear wall is higher than that of coupling beam so that with an increase in the height, we see a 41.6% increase in the energy dissipation of the coupling beam, while this upward trend is 45% in the case of steel plate shear wall. According to Fig. 10, with increasing the frame height, the ductility of coupling beam increases while the ductility of steel plate shear wall decreases. The increase rate in the ductility of coupling beam has increased by 40% for a 24 m increase in the height of the frame, and the decrease rate in the ductility of steel plate shear wall has increased by 21% for the same amount of increase in the height of the frame. In Table 5, the numerical values of ductility and energy dissipation of the coupling beam and steel plate shear wall in different modes of modeling are presented and compared with the numerical values provided by Pavir and Shekastehband [7].

Based on the study conducted by Pavir and Shekastehband [7], it is possible to provide the shear capacity of

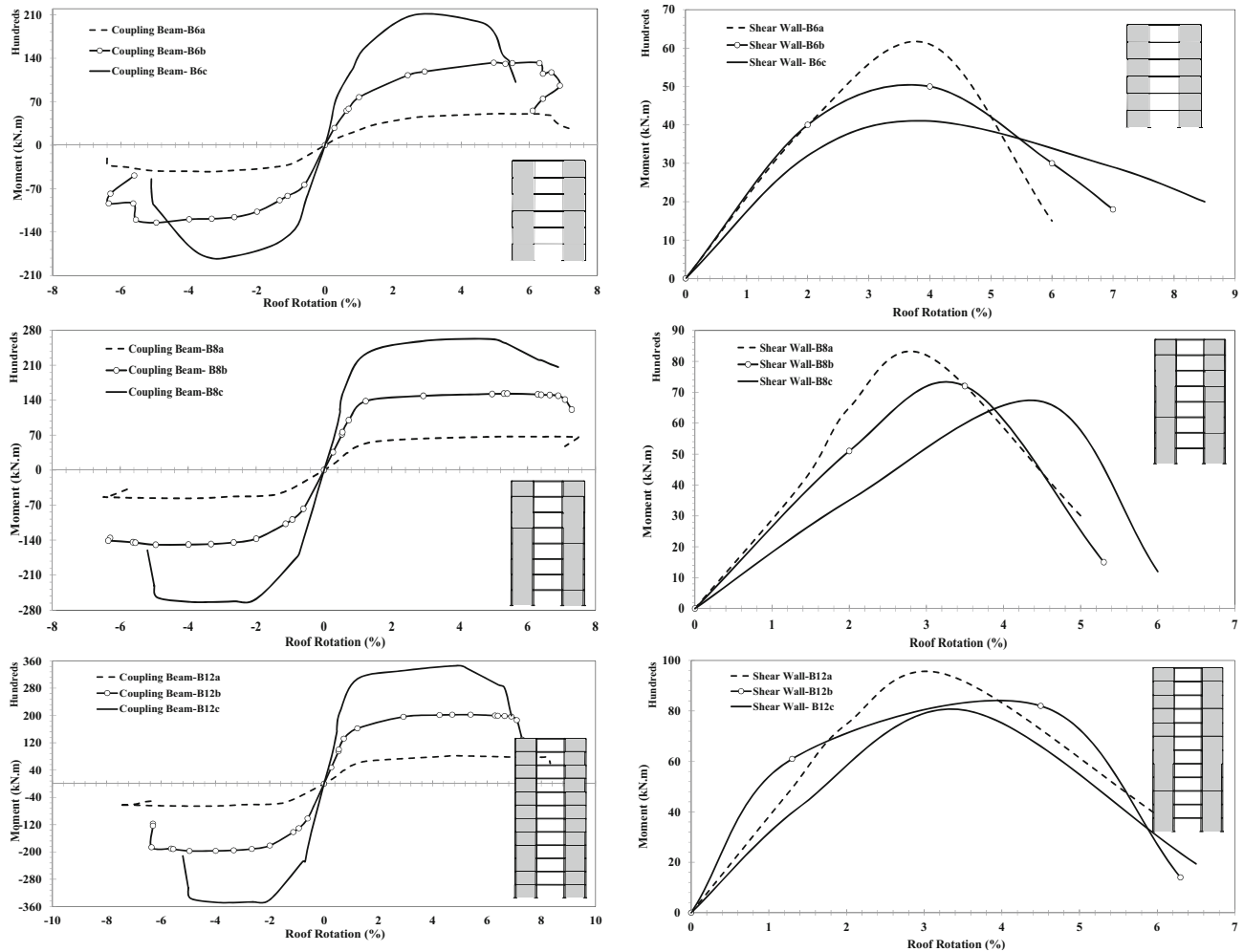


**Fig. 8** Comparison of bending moment–rotation hysteresis curve envelope of coupling beam and shear wall of six-, eight- and twelve-story frames in different models

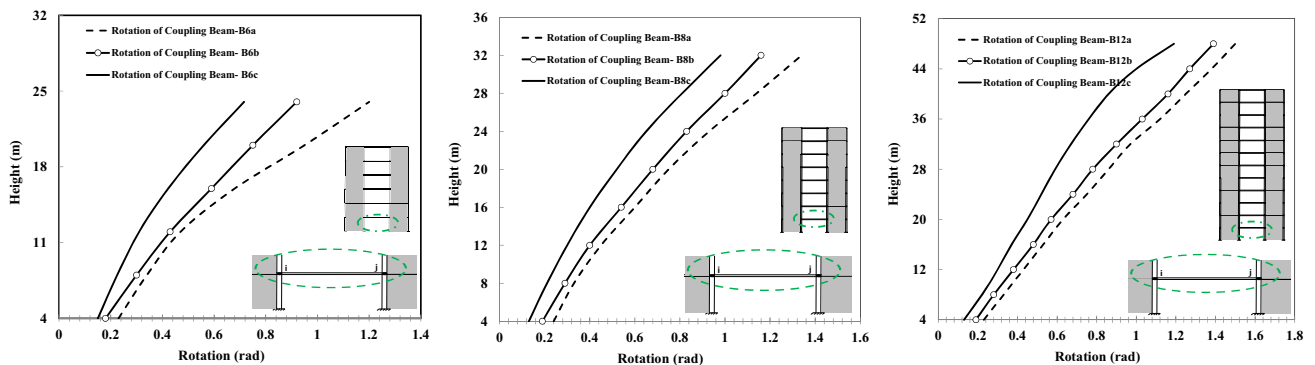


**Fig. 9** Comparison of the coupling beam rotation of six-(left), eight-(middle) and twelve-(right) story frames in different conditions

coupled steel plate shear wall based on Eq. (5). The total shear capacity of columns and coupling beams can be calculated according to Eq. (6), and the shear capacity of steel plate shear wall can be calculated according to Eq. (7). In this equation,  $V_{SC}$  is final shear capacity of coupled steel plate shear wall,  $V_c$  is the shear capacity of

column,  $V_p$  is the shear capacity of steel plate shear wall,  $V_{CB}$  is the shear capacity of coupling beam,  $h_i$  is the story height,  $MP_{(EVBEi)}$  is the plastic moment of outer column,  $MP_{(IVBEi)}$  is the plastic moment of inner column,  $MP_{(CB)}$  is the plastic moment of coupling beam,  $L$  is the span length,  $e$  is the length of coupling beam,  $F_{yp}$ ,  $t$ , and  $L_p$ ,



**Table 5** Numerical parameters for modeling the CSSHL2 model [7]

	4 story Pavir and Shekasteband [7]		6 story (present research)		8 story (present research)		12 story (present research)	
	Coupling beam	Shear wall	Coupling beam	Shear wall	Coupling beam	Shear wall	Coupling beam	Shear wall
Energy (kN.m)	3530	1410	3961	1565	4838	2202	6785	2861
Ductility	4.204	3.9	4.502	3.18	6.2	2.7	6.63	2.5

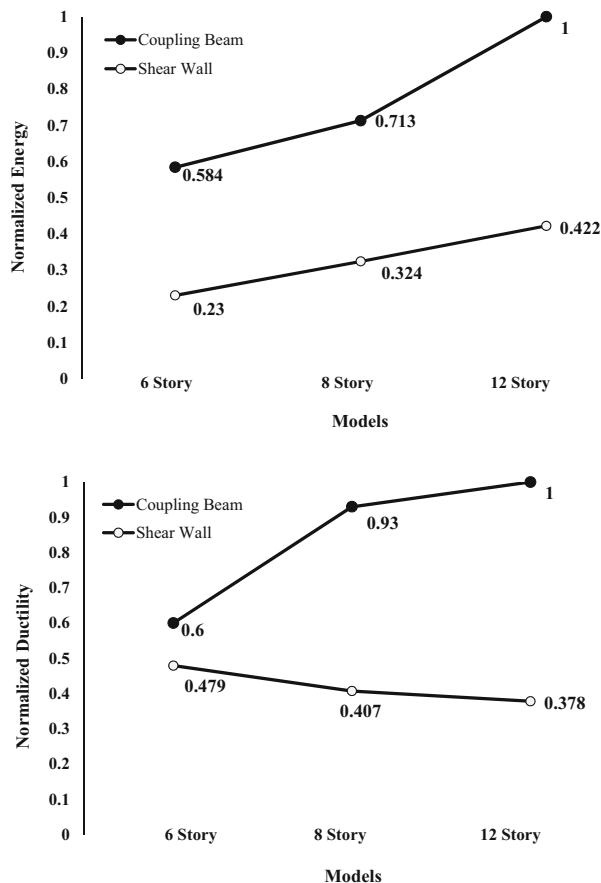


**Fig. 10** Comparison of ductility and normalized energy of coupling beam and shear wall in six-, eight- and twelve-story frames

respectively, are the yield stress, the thickness, and the length of equivalent steel diagonal strip, and  $\alpha$  is the slope of angle between the equivalent steel diagonal strip with horizon [7].

$$V_{sc} = V_c + V_p + V_{cB} \tag{5}$$

$$V_c + V_{cB} = \left( 1 / \sum_{i=1}^n h_i \right) \times \left[ (2M_{P(EVBEi)} + 2M_{P(IVBEi)} + 2M_{P(CB)}) \times \left( \frac{e+l}{e} \right) \right] \tag{6}$$

$$V_p = \frac{1}{2} F_{yp} t L_p \sin(2\alpha) \tag{7}$$

Based on the results obtained from the present study and according to the information presented in Table 6, the length of coupling beam affects the shear capacity of the steel plate shear wall. Therefore, in this section, we seek to provide parametric relationships regarding the calculation of the shear capacity of steel plate shear wall depending on the length of coupling beam. Due to the fact that some parameters are fixed in Eq. (7), like the yield stress of shear wall ( $F_{yp}$ ) equal to 25,720 kN/m<sup>2</sup>, the thickness of shear wall ( $t$ ) equal to 1 mm, the angle between the horizon and the diagonal element of the shear wall ( $\alpha$ ) equal to 51 degrees, and finally the length of equivalent diagonal element of shear wall ( $L_p$ ) equal to 5.12 m, the shear capacity of the steel plate shear wall can be rewritten based on Eq. (9). The coefficient  $\alpha_2$  can be calculated according to Eq. (8) with respect to the length of equivalent diagonal strip ( $L_p$ ) and the length of coupling beam ( $L_{CB}$ ).

$$L_p = \alpha_2 L_{CB} \tag{8}$$

$$V_p = \frac{1}{2} F_{yp} \alpha_1 \alpha_2 L_{CB} t \sin(2\theta) \tag{9}$$

Using Eq. (9), the numerical values of the coefficient  $\alpha_1$  are obtained according to Table 7. With respect to Fig. 11, the line equation for determining the coefficient  $\alpha_1$  in terms of the length of coupling beam for the six-, eight- and twelve-story frames using nonlinear regression, and for generalizing the aforementioned relation, different frames from 3 to 60 m with an increase step of three meters (20 frames) was evaluated and the general line equation for determining the coefficient  $\alpha_1$  in terms of the length of the coupling beam is presented based on Eq. (10). Table 8 presents the numerical values of the coefficient  $\alpha_1$  for three different lengths of coupling beam for the 20 frames under study. Figure 12 shows the variation of error (coefficient  $\alpha_1$ ) in terms of the Neperian logarithm of the squared values for different coupling beam length. As can be seen, the appropriate distribution of data in Fig. 12 indicates the acceptable accuracy of the relation for determining the coefficient  $\alpha_1$  in terms of changes in the coupling beam length and the frame height (Eq. (10)).

$$\alpha_1 = -0.3471 L_{CB}^2 + 2.3421 L_{CB} + 2.5 \tag{10}$$

By placing Eq. (10) in Eq. (9), the equation for determining the shear capacity of the steel plate shear wall

**Table 6** Maximum shear capacity of steel plate shear wall ( $V_P$ (kN)) for different lengths of coupling beam

Length of CB (m)	Frame height		
	$H = 24$ m	$H = 32$ m	$H = 48$ m
$L = 1.65$	3155	4732	5679
$L = 3.5$	3055	4632	5527
$L = 5$	2655	4430	5115

**Table 7** Coefficient  $\alpha_1$  to calculate the shear capacity of steel plate shear wall

	0.5 $F_{yp}$	$L_{cb}$	$t$	$\sin(2\theta)$	$V_p$	$\alpha_2$	$\alpha_1$	
$H = 24$	$L = 1.65$	128,600	1.65	0.001	0.978	3155	3.1	4.9
	$L = 3.5$	128,600	3.5	0.001	0.978	3055	1.46	4.75
	$L = 5$	128,600	5	0.001	0.978	2655	1.024	4.12
$H = 32$	$L = 1.65$	128,600	1.65	0.001	0.978	4732	3.1	7.35
	$L = 3.5$	128,600	3.5	0.001	0.978	4632	1.46	7.2
	$L = 5$	128,600	5	0.001	0.978	4430	1.024	6.87
$H = 48$	$L = 1.65$	128,600	1.65	0.001	0.978	5679	3.1	8.83
	$L = 3.5$	128,600	3.5	0.001	0.978	5227	1.46	8.13
	$L = 5$	128,600	5	0.001	0.978	5115	1.024	7.94

**Table 8** Coefficient  $\alpha_1$  for three different lengths of coupling beams for 20 frames

Frame height (m)	LCB = 1.65	LCB = 3.5	LCB = 5
3	2.12	2.01	1.85
6	2.5	2.33	1.92
9	2.92	2.64	2.06
12	3.2	2.98	2.37
15	3.7	3.3	2.95
18	4.2	3.95	3.4
21	4.5	4.36	3.74
24	4.9	4.75	4.12
27	6.4	5.8	4.72
30	6.83	6	5.6
33	7.4	7.25	6.9
36	7.73	7.38	6.98
39	7.91	7.68	7.09
42	8.23	7.83	7.25
45	8.46	7.99	7.6
48	8.83	8.13	7.94
51	8.9	8.2	7.98
54	8.97	8.29	8.06
57	9.05	8.46	8.21
60	9.1	8.67	8.37

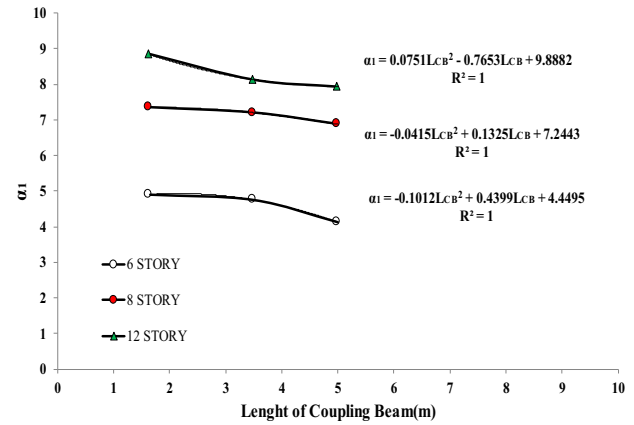


**Fig. 11** The line equation for determining the coefficient  $\alpha_1$  in terms of the length of coupling beam in six-, eight- and twelve-story frame

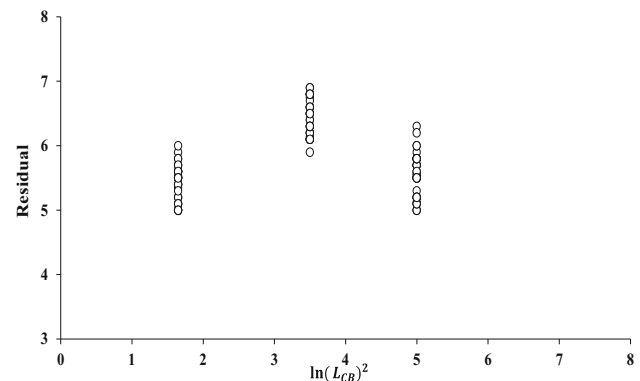


**Fig. 12** Variation of error in terms of the Neperian logarithm of the squared values for different coupling beam length

based on the coupling beam length can be expressed through Eq. (11).

$$V_P = F_{yp} \sin(2\theta) t \alpha_2 [-0.174 L_{CB}^3 + 1.17 L_{CB}^2 + 1.25 L_{CB}] \tag{11}$$

**Conclusion**

In this study, the main purpose is to investigate the behavior of the components of coupled steel plate shear wall (coupling beam and steel plate shear wall) under cyclic loading.

Comparing the results of applying one cyclic load, it was observed that.

- (i) By changing the length of coupling beam, the shear capacity, flexural capacity, ductility and energy dissipation in the components of the coupled steel plate shear walls change significantly, in such a way that increasing the length of coupling beam increases and decreases the aforementioned parameters regarding coupling beam and steel plate shear wall, respectively.

- (ii) In addition to the length of coupling beam, the height of frame can also have a significant effect on the responses obtained under cyclic load, in such a way that increasing the height of frame increases the rotation recorded in coupling beam, and by increasing the length of coupling beam, the rotations created in coupling beam have been decreased and the increasing rate of rotation in coupling beam increases as the height of frame rises.
- (iii) In this study, due to the significant effect of coupling beam length parameter, the shear capacity equation of the steel plate shear wall has been rewritten based on coupling beam length variable.

**Funding** The authors have not disclosed any funding.

#### Declarations

**Conflict of interest** The authors have not disclosed any conflict of interest.

#### References

- M. Gholhaki, H. AsghariTakdam, Investigating the nonlinear dynamic behavior of steel plate shear wall with thin plate having a beam connecting to rigid column under near- and far-fault mappings. *Ferdowsi J. Civ. Eng.* **26**(1), 63–84 (2014)
- W.S. Park, H.D. Yun, Seismic behavior of coupling beams in a hybrid coupled shear walls. *J. Constr. Steel Res.* **61**(11), 1492–1524 (2005)
- M. Gholizadeh, Y. Yadollahi, *The effect of wave density on the behavior of steel plate shear walls with corrugated plates*. In: sixth national congress of civil engineering, Semnan university, Semnan, (2011)
- A. Eljadei, *Performance based design of coupled wall structures*. Doctor of Philosophy, University of Pittsburgh (2012)
- H.A. Mazaheri, M.R. Shekari, *Investigating the performance of coupled steel plate shear wall with boundary beam with reduced cross section*. In: national conference on basic research in civil engineering, architecture and urban planning, Tehran, Ouj higher education institute (2018)
- M.S. Hoehler, C.M. Smith, T.C. Hutchinson, X. Wang, B.J. Meacham, P. Kamath, Behavior of steel-sheathed shear walls subjected to seismic and fire loads. *Fire Saf. J.* **91**, 541–531 (2017)
- A. Pavir, B. Shekastehband, Hysteretic behavior of coupled steel plate shear walls. *J. Constr. Steel Res.* **133**, 19–35 (2017)
- H.S. Hu, J.G. Nie, M.R. Eatherton, Deformation capacity of concrete-filled steel plate composite shear walls. *J. Constr. Steel Res.* **103**, 148–158 (2014)
- D. Dan, A. Fabian, V. Stoian, Theoretical and experimental study on composite steel–concrete shear walls with vertical steel encased profiles. *J. Constr. Steel Res.* **67**(5), 800–813 (2011)
- D.J. Borello, L.A. Fahnestock, Behavior and mechanisms of steel plate shear walls with coupling. *J. Constr. Steel Res.* **74**, 8–16 (2012)
- D.J. Borello, L.A. Fahnestock, Design and testing of coupled steel plate shear walls. *Struct. Congr.* **2011**, 736–747 (2011)
- J. Berman, S. Bruneau, Plastic analysis and design of steel of plate shear walls. *J. Struct. Eng.* **129**(11), 1448–1456 (2003)
- M. Gholhaki, M.B. Ghadaksaz, Investigation of the link beam length of a coupled steel plate shear wall. *Steel Compos. Struct.* **20**(1), 107–125 (2016)
- M. Safari Gorji, J.J.R. Cheng, Steel plate shear walls with outriggers. Part I: plastic analysis and behavior. *J. Constr. Steel Res.* **134**, 148–159 (2017)
- M. Safari Gorji, J.J.R. Cheng, Steel plate shear walls with outriggers. Part II: seismic design and performance. *J. Constr. Steel Res.* **137**, 311–324 (2017)
- M. Safari Gorji, J.J.R. Cheng, Seismic behavior of coupled steel plate shear walls with simple boundary frame connections. *Earthq. Eng. Struct. Dyn.* **48**, 1–21 (2018)
- ANSI/AISC 341 An American National Standard.341-16 *Seismic provisions for structural steel building*, American institute for steel construction 130 East Randolph Street Suite, 2000 Chicago Illinois 60601-6204 (2016)
- ASCE. *Minimum design loads for building and other structures* (ASCE/SEI 7-10), American Society of Civil Engineers (2010)
- J. Vaseghi Amiri, M. Hosseinali Beigi, I. Mohammadpour Nikbin, *Steel plate shear walls (performance, analysis and design)*. Babol: Babol Noshirvani University of Technology Press (2011)
- S. El-Tawil, C.M. Kuenzli, Pushover of hybrid coupled walls. II: analysis and behavior. *J. Struct. Eng.* **128**(10), 1282–1289 (2002)
- R.G. Driver, G.L. Kulak, D.L. Kennedy, A.E. Elwi, Cyclic test of four-story steel plate shear wall. *J. Struct. Eng.* **124**(2), 112–120 (1998)
- PEER. *Open system for earthquake engineering* (OpenSees). Version2.4.0, Berkeley: Pacific Earthquake Eng, Research Center, University of California (2005)
- K.A. Harries, D. Mitchell, W.D. Cook, Seismic response of steel beams coupling concrete walls. *J. Struct. Eng.* **119**(12), 3611–3629 (1993)
- K.A. Harries, D. Mitchell, R.G. Redwood, Nonlinear seismic response predictions of walls coupled with steel and concrete beams. *J. Civ. Eng.* **25**(5), 803–818 (1998)
- Venture, SAC Joint. *Protocol for fabrication, inspection, testing and documentation of beam-column connection tests and other experimental specimens*, Rep. No. SAC/BD-97 (1997)
- T. White, P. Adebar, *Estimating rotational demands in high-rise concrete wall buildings*. In: 13th world conference on earthquake engineering, Vancouver, B.C, Canada (2004)

**Publisher's Note** Springer Nature remains neutral with regard to jurisdictional claims in published maps and institutional affiliations.